View metadata, citation and similar papers at core.ac.uk
brought to you by CORE
provided by The University of Utah: J. Willard Marriott Digital Library



# Sub-10 nm lateral spatial resolution in scanning capacitance microscopy achieved with solid platinum probes

E. Bussmann and C. C. Williams[a]
*Department of Physics, University of Utah, 115 S 1400 E, Room 201, Salt Lake City, Utah 84112*

(Received 15 September 2003; accepted 26 October 2003)

Sub-10 nm resolution can be obtained in scanning capacitance microscopy (SCM) if the probe tip is approximately of the same size. Such resolution is observed, although infrequently, with present commercially available probes. To acquire routine sub-10 nm resolution, a solid Pt metal probe has been developed with a sub-10 nm tip radius. The probe is demonstrated by SCM imaging on a cross-sectioned 70 nm gatelength field-effect transistor (FET), a shallow implant ($n^+/p$, 24 nm junction depth), and an epitaxial staircase ($p$, ~75 nm steps). Sub-10 nm resolution is demonstrated on the FET device over the abrupt meeting between a silicon-on-insulator oxide layer and a neighboring Si region. Comparable resolution is observed on the implant structure, and quantitative SCM dopant profiling is performed on it with sub-10 nm accuracy. Finally, the epitaxial staircase structure is quantitatively profiled demonstrating the accuracy obtained in quantitative profiling with the tips. © *2004 American Institute of Physics.* [DOI: 10.1063/1.1641161]

## I. INTRODUCTION

Scanning capacitance microscopy (SCM) is a technique which may be used for two-dimensional dopant profiling in semiconductors.[1] A conductive atomic force microscope (AFM) probe is scanned in contact mode over a surface while a resonant capacitance sensitive circuit is used to sense capacitance variations. When applied to a semiconductor surface (Si) with a dielectric film ($SiO_2$) on the surface, the probe–dielectric–semiconductor forms a metal–insulator–semiconductor (MIS) capacitor. In the case of the metal–$SiO_2$–Si structure, the one dimensional $C-V$ curves are known from theory.[2] In the constant $\Delta V$ mode, the SCM sensor can be tuned with applied voltages to have an output proportional to the slope of the local $C-V$ curve near its inflection point (approximately the MIS flatband voltage, $V_{fb}$).[1] The slope of the $C-V$ curve around $V_{fb}$ is related to the activated doping of the semiconductor. With adequate surface preparation and biasing, the SCM signal decreases monotonically with increasing dopant and carrier concentration over a range of dopant concentrations from about $10^{15}-10^{20}/cm^3$.[3]

The SCM has lateral spatial resolution and depth spatial resolution. In the context of this article, SCM lateral spatial resolution is the length for the SCM signal to change from 10% to 90% of full signal near the abrupt meeting of two materials which yield different SCM signal sizes. SCM spatial resolution is limited by the carrier depleted volume of the semiconductor in the measurement.[4] The probed volume depends on the probe tip radius and shape and the applied voltages.[5] Depth resolution is generally not problematic since device structures are generally much deeper than the depth of the depletion in the semiconductor. The lateral resolution of the SCM is improved by reducing the size of the probe.

Typical probes with a metal coating have tip radii of 15–35 nm.[6] The lateral distance to resolve an oxide structure from an adjacent doped region is somewhere between a tip radius and a tip diameter as predicted by our SCM model (DPACK 3.0).[7] Theoretical models predict SCM can achieve spatial resolution below 10 nm with accuracy on a similar scale.[8,9] Such results can occasionally be obtained with presently available AFM tip technology. However, a probe with a regular sub-10 nm end radius is required for obtaining sub-10 nm resolution and accuracy on a routine basis.

Various probe technologies have properties which limit their reliability, or make them less desirable candidates for regular sub-10 nm tip size. A discussion and analysis of various probe technologies is found in the article by Trenkler *et al.*[10] Sub-10 nm probes of doped Si have been used, but they may have (low quality) native oxides on their surface. In addition, being made of doped Si, they contribute their own $C-V$ characteristics to the measured signal.[11] Metal coated Si probes have been used successfully, but problems including wear and eventual deadherence of the metal coatings have been observed in our laboratory, and reported by others.[12] Diamond coated cantilevers show good wear properties.[13] Metal coated Si cantilevers are prepared from a substrate material ($Si, Si_3N_4$) to a sharp point, then coated in conductive material (Pt–Ir, Pt–Cr). Then the probe has a tip radius no less than the thickness of the conductive coat. In these regards, a solid metal tip is advantageous, since it will not suffer from semiconductor depletion effects and sudden loss of conductivity due to the deadherence of a metal coating. A solid metal probe tip technology with a sub-50 nm probe tip is described in the article by Yamamoto *et al.*[12]

A probe with a tip of solid platinum metal with a sub-10 nm end radius has been constructed. It is currently being prepared for commercial availability. The resolution of the

[a]Author to whom correspondence should be addressed; electronic mail: clayton@physics.utah.edu

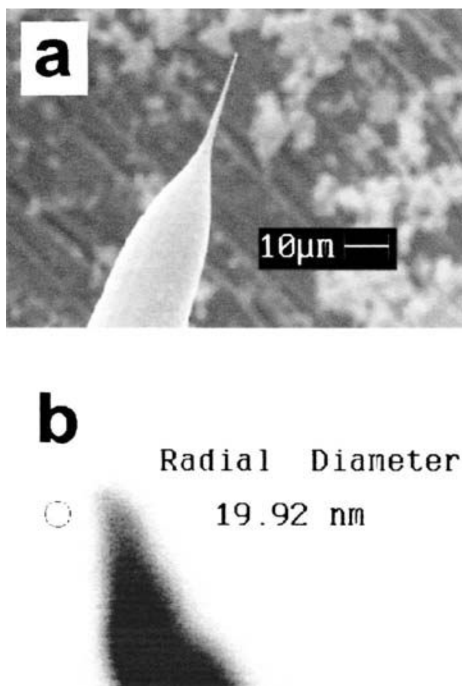


FIG. 1. (a) SEM image of the usual tip geometry. (b) The small scale (~10 nm) geometry of the tip imaged by SEM. A circle of 19.92 nm diameter is shown as a scale to aid the eye.

tip has been evaluated by SCM imaging of small structures in cross section. Sub-10 nm resolution is demonstrated on two structures: a 70 nm gatelength silicon-on-insulator field-effect transistor (SOI FET) device and a shallow implant ($n^+/p$, 24 nm junction depth). In each case, the measured SCM signal is compared with modeled SCM responses from secondary ion mass spectroscopy (SIMS) dopant data using DPACK 3.0. A quantitative dopant profile from the measured SCM data is demonstrated for the latter structure. The quantitative dopant profile is accurate on a sub-10 nm scale, and agrees with SIMS data on this scale. However, the incomplete junction model used prevents accurate dopant profiling within about one tip radius of junction regions. Finally, an epitaxial staircase structure ($p$, ~75 nm steps) has been prepared and imaged with high resolution (although not sub-10 nm) to evaluate the quantitative accuracy of SCM profiles obtained with the Pt tips.

## II. PROBE PREPARATION AND PROPERTIES

The probes are fashioned from platinum metal wire. The cantilever arm is 0.5–1 mm long. The probe tip is prepared by electrochemical etching, and subsequent fine polishing.[14,15] Probe tips have 10 nm or smaller radii in roughly 50% of cases by this method. The tips are characterized by a scanning electron microscope. Figure 1 shows a typical probe shape and tip profile.

The probes must have low force constants (~0.2 N/m) to maintain low wear in contact mode. The natural frequency of the cantilever arms is generally 20–50 kHz, so the probes may also be used for electrostatic force microscopy or tapping mode AFM in this frequency range. The probes are found to wear to larger radii after about 25 complete 1 $\mu m^2$ images (128 scans per image) on a polished Si surface with

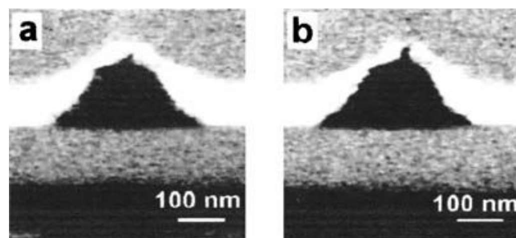


FIG. 2. Images of a 70 nm gatelength SOI FET device. (a) The sample has been held at a dc bias of −2 V with respect to the flatband voltage and the apparent electrical junctions around the source/drain extensions shift inward. (b) The sample has been held at +1 V with respect to the flatband potential and the source/drain extensions recede.

0.2 to 0.3 nm rms roughness. Transition lengths across the abrupt meeting of oxide and doped Si increase gradually from sub-10 nm to ~15 nm over this number of scans. The lifetime of the tip may be increased by reducing the force constant of the cantilever and reducing the force set-point of the AFM feedback loop.

## III. SCM METHOD

The SCM imaging is performed with a Digital Instruments 3000 AFM. The capacitance sensor is a modified RCA sensor.[16] This sensor has a demonstrated sensitivity of 1.5 $\times 10^{-21}$ F/Hz$^{1/2}$. The sensor consists of a resonant circuit ($f_o \sim 700$ MHz, $Q \sim 40$), driven by a rf voltage of 1 V amplitude, tuned near resonance. An ac voltage (1 V amplitude, 50 kHz) is applied to the sample. In addition, a variable dc voltage ($-2$ V$<V_{dc}<2$ V) for biasing the sample to the flatband condition is applied. The amplitude and sign of all three voltages plays some part in the resolution and accuracy of the SCM. The tuning of the resonant circuit also effects the spatial resolution.[7]

The sample cross sections are prepared for SCM by polishing on diamond embedded pads of decreasing grit size between 3 and 0.05 $\mu$m. The surface is then chemically oxidized on a cloth pad saturated with KOH:colloidal silica ($p$H~11) in $H_2O$:$NH_4OH$:$H_2O_2$ (10:1:1, by volume) solution. The rms roughness of the surface is generally 0.1–0.3 nm after the polishing. The surface is further prepared by annealing at 300 °C for 30 min under UV illumination, as this has been determined to improve the SCM signal.[11] Optimization of the surface response is critical because the SCM signal drops with the area of the tip. With tips of small size, background noise becomes more significant. The signal-to-noise ratio is at best ~20 ($\tau$=3 ms, imaging with the modified RCA sensor) in images acquired with the Pt probes on Si doped at $10^{18}$/cm$^3$–$10^{19}$/cm$^3$ with oxides grown and prepared by the method described previously.

## IV. FET DEVICE IMAGING

A 70 nm gatelength silicon-on-insulator (SOI) field-effect transistor (FET) has been prepared and imaged by SCM in cross section. High resolution images of the device are presented in Fig. 2 (500 nm square images, 128 samples per line). In Fig. 2(a), a −2 V dc bias (with respect to channel flatband voltage) has been applied, and the source/drain extensions shift inward and appear to meet in the channel.

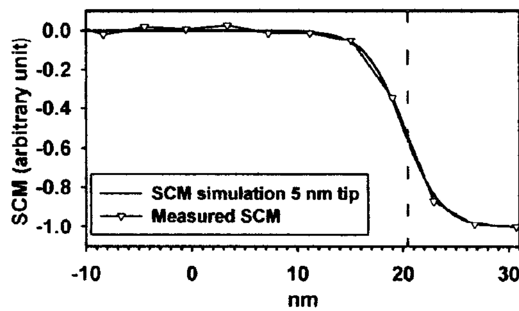


FIG. 3. The discrete SCM sampling over the transition region from the SOI layer (left) to channel region (right). The measured SCM is the mean of ten individual measurements to suppress noise. The transition length is in agreement with that simulated for a 5 nm tip. The dotted vertical line indicates the junction between the SOI layer (left) and the doped channel region (right).

The effect is due to bending of the majority carrier edge by the applied bias.[17] In Fig. 2(b), a bias of +1 V (with respect to channel flatband voltage) has been applied to the sample, and the source/drain extensions recede due to the same effect with the opposite sign of voltage. Note that the channel region in Fig. 2(b) has been resolved at ~24 nm (separation between apparent electrical junctions) with about 60%–70% full signal as compared with the region just below the channel. In addition, the resolution permits clear imaging of the source/drain extensions.

The transition length from the oxide layer below the device to the doped channel region is taken as a measure of the resolution. The SCM model gives the transition length (10%–90% of full signal) to be somewhat larger (1 to 2×) than the tip radius under the imaging conditions. The mean (to suppress noise) of ten measured SCM signals over this transition, taken in the fast scan direction, is shown with the simulated SCM signal in Fig. 3. The transition length from 10% to 90% full signal is ~8 nm. Assuming channel doping in the near vicinity of the SOI layer in the $10^{18}$–$10^{19}$/cm$^3$ range, the agreement between the model SCM and the measured SCM suggests a tip with a 5–7.5 nm radius.

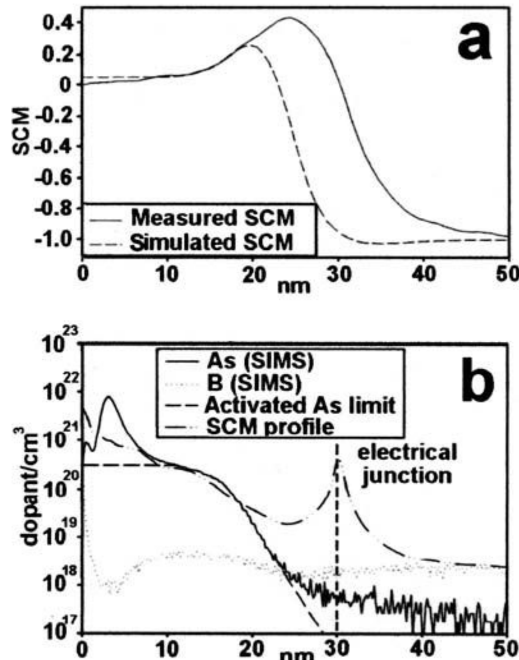


FIG. 4. (a) Measured SCM and simulated SCM for 8.5 nm radius tip on sample 1 ($n^+/p$, 24 nm junction depth). The simulation calculates capacitance based on the dopant profile, so it becomes inaccurate in the junction region where the carrier and dopant profiles diverge. The simulation predicts an apparent electrical junction (SCM zero signal crossing) very near the metallurgical junction depth (~24 nm). (b) The overlain SIMS and SCM dopant profiles. The spike in the SCM profile near the left edge is a consequence of the slightly lower SCM signal measured near the edge due to the influence of the $a$-Si layer there. The spike in the center of the SCM profile (~29 nm depth) is a consequence of the SCM conversion model which is not adequate to handle the junction.

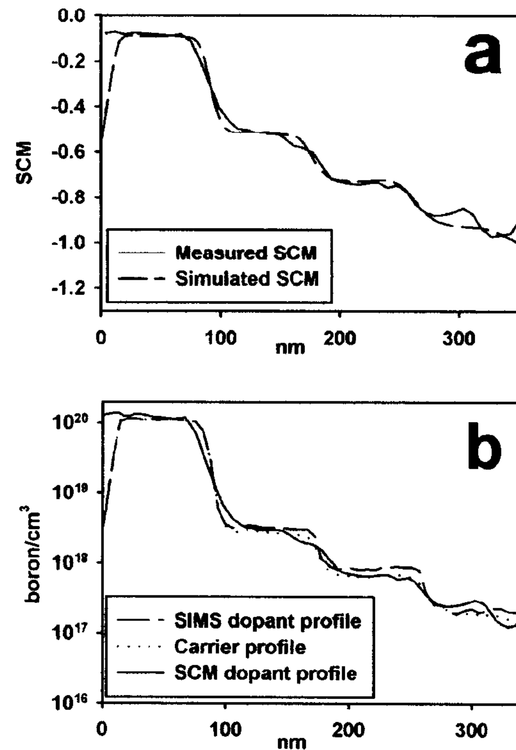


FIG. 5. (a) Measured SCM and simulated SCM (10 nm tip radius) for the four step boron epitaxial staircase structure with ~75 nm steps. The resolution in this case is not as high as expected for a sub-10 nm tip radius, probably due to both larger tip radius and rf voltage. (b) The SCM dopant profile and SIMS profile for the epitaxial staircase sample.

## V. SHALLOW IMPLANT IMAGING

A shallow implant ($n^+/p$, 24 nm junction depth) has been prepared and imaged by SCM. The implant was characterized by secondary ion mass spectroscopy (SIMS) to determine the dopant depth profile. The implant is at the wafer top surface, so the sample was sputter coated with a layer of $a$-Si ($n$,$10^{19}$/cm$^3$) to about 1 $\mu$m depth to protect it during polishing. The sample was then polished and prepared for imaging.

Square SCM images of 100 or 200 nm size sampled at 128 samples/line (100 nm images) or 256 samples/line (200 nm images) have been acquired with the platinum probes on the sample. The SCM signal size varies by about 10% on a 10 nm lateral scale from line to line, probably due to changing surface properties, such as oxide thickness or defect density. Further, surface noise and electrical noise are present, and are more dominant with smaller tips.[18] For these reasons,

a number of SCM lines spaced evenly across each image have been averaged to give a characteristic quantitative SCM line.

Figure 4(a) shows the fit between simulated and measured SCM lines. Good agreement is seen from 8 to 20 nm in the center of the profiles. The measured SCM is different from the model SCM from 0 to 8 nm at the left of the image (approximately one tip radius, 8.5 nm, from the sputtered $a$-Si layer). This difference may be due to the influence of the $a$-Si on the $C-V$ response there. The signals are also different from 20 to 40 nm since the model used for SCM simulation does not accurately model the junction. The model SCM uses the SIMS doping profile to calculate the SCM profile, while the SCM responds to the carrier profile.

In Fig. 4(b), the SCM line of Fig. 4(a) has been converted to a dopant profile. The SIMS data is illustrated with modified SIMS data where the doping level is cutoff at $3 \times 10^{20}/\mathrm{cm}^3$ (the limit set by the solid solubility of As in Si).[19] The small difference between the measured and modeled SCM signals over the range from 0 to 8 nm in Fig. 4(a) converts to a large difference between the SIMS and the SCM dopant profiles. The spike in the center of the SCM dopant profile is a result of the simplified junction model which cannot distinguish the convolution of $n$- and $p$-type responses in the junction region from an extremely high doping level. The SCM measures an apparent electrical junction (SCM zero signal) much nearer to the true electrical junction, established by diffusion and drift current equilibrium, than to the SIMS metallurgical junction. The metallurgical junction lies at 24 nm in SIMS data, while the carrier equilibrium distribution places the electrical junction at 30 nm. The apparent electrical junction (SCM zero signal) is at $29 \pm 3$ nm.

## VI. EPITAXIAL STAIRCASE IMAGING

An epitaxial staircase structure has been imaged to demonstrate that quantitative accuracy can be achieved with the Pt probes on a nonjunction structure with a transition between two doping levels. The epitaxial layers do not have atomically abrupt transitions according to the SIMS data. The sample was prepared by evaporation of 80 nm Cr onto the top surface, then sputtering of $\sim 1$ $\mu$m of Si$(n, 10^{19}/\mathrm{cm}^3)$. The sample surface was polished and prepared by the methods described earlier.

The measured SCM signal is shown in Fig. 5(a) with the simulated SCM signal for a 10 nm tip radius. Sub-10 nm resolution was not obtained on this structure. This may be due to a large rf voltage to improve the signal-to-noise ratio, or a large tip end radius. The measured SCM doping profile is shown in Fig. 5(b) with the SIMS data and carrier profile. The SCM profile is in close agreement with the carrier profile over the first three steps. There is sub-10 nm disparity between the measured SIMS data, carrier profile, and the SCM dopant profile in the transition regions between steps.

## VII. DISCUSSION

Reliable characterization and dopant profiling of sub-50 nm devices and ultrashallow implants by scanned probe techniques will require extremely sharp metallic probes with good wear properties. Solid Pt metal probes are sufficiently robust for repeated imaging on a sub-$\mu$m scale. Combined with edge registration techniques, and modeling of the SCM signal, sub-5 nm accuracy is achievable with agreement to SIMS profiles on the same scale. Progress toward sub-5 nm SCM resolution will include optimization of the imaging parameters and further improvement of the probe fabrication process. In addition, capacitance sensors must be improved for use with sub-10 nm tips.

## ACKNOWLEDGMENTS

Research funded by SRC. Thanks to P. Ronsheim, IBM, for all the samples.


[1] C. C. Williams, Annu. Rev. Mater. Sci. **29**, 471 (1999).
[2] S. M. Sze, *Physics of Semiconductor Devices*, 2nd ed. (Wiley New York, 1981).
[3] T. Clarysse, M. Caymax, P. De Wolf, T. Trenkler, W. Vandevorst, J. S. McMurray, J. Kim, C. C. Williams, J. G. Clark, and G. Neubauer, J. Vac. Sci. Technol. B **16**, 394 (1998).
[4] J. J. Kopanski, J. F. Marchiando, and J. R. Lowney, J. Vac. Sci. Technol. B **14**, 242 (1996).
[5] J. J. Kopanski, J. F. Marchiando, and B. G. Rennex, J. Vac. Sci. Technol. B **20**, 2101 (2002).
[6] MikroMasch Ultrasharp CSC17/Pt.
[7] J. S. McMurray, Ph.D. dissertation, University of Utah, 2000.
[8] H. P. Kleinknecht, J. R. Sandercock, and H. Meier, Scanning Microsc. **2**, 1839 (1988).
[9] Š. Lanyi and M. Hruškovic, J. Phys. D **36**, 598 (2003).
[10] T. Trenkler, T. Hantschel, R. Stephenson, P. De Wolf, W. Vandervorst, L. Hellemans, A. Malavé, D. Büchel, E. Oestershulze, W. Kulische, P. Niedermann, T. Sulzbach, and O. Ohlsson, J. Vac. Sci. Technol. B **18**, 418 (2000).
[11] V. V. Zavyalov, J. S. McMurray, and C. C. Williams, Rev. Sci. Instrum. **70**, 158 (1999).
[12] T. Yamamoto, Y. Suzuki, M. Miyashita, H. Sugimura, and N. Nakagiri, J. Vac. Sci. Technol. B **15**, 1547 (1997).
[13] H. Yabuhara, M. Ciappa, and W. Fichtner, J. Vac. Sci. Technol. B **20**, 783 (2002).
[14] A. J. Melmed, J. Vac. Sci. Technol. B **9**, 601 (1991).
[15] L. Libioulle, Y. Houbion, and J.-M. Gilles, J. Vac. Sci. Technol. B **13**, 1325 (1995).
[16] J. S. McMurray and C. C. Williams, Proceedings of the Sixth International Workshop on Fabrication, Characterization, and Modeling of Ultra-Shallow Doping Profiles in Semiconductors, Napa, CA, 2001, p. 199.
[17] H. Edwards, R. McGlothin, R. San Martin, E. U, M. Gribelyuk, R. Mahaffy, C. Ken Shih, R. Scott List, and V. Ukraintsev, Appl. Phys. Lett. **72**, 698 (1998).
[18] V. V. Zavyalov, J. S. McMurray, and C. C. Williams, J. Vac. Sci. Technol. B **18**, 1125 (2000).
[19] A. Nylandsted Larsen, S. Yu. Shiryaev, and E. Schwartz Sørensen, Appl. Phys. Lett. **48**, 1805 (1986).

Review of Scientific Instruments is copyrighted by the American Institute of Physics (AIP). Redistribution of journal material is subject to the AIP online journal license and/or AIP copyright. For more information, see http://ojps.aip.org/rsio/rsicr.jsp
Copyright of Review of Scientific Instruments is the property of American Institute of Physics and its content may not be copied or emailed to multiple sites or posted to a listserv without the copyright holder's express written permission. However, users may print, download, or email articles for individual use.